How should leaf area, sapwood area and stomatal conductance vary with tree height to maximize growth?

THOMAS N. BUCKLEY[1–3] and DAVID W. ROBERTS[4]

[1] *Environmental Biology Group and CRC for Greenhouse Accounting, Research School of Biological Sciences, The Australian National University, Canberra, ACT 2601, Australia*

[2] *Present address: Biology Department, Utah State University, Logan, UT 84322, USA*

[3] *Corresponding author (tom_buckley@alumni.jmu.edu)*

[4] *Ecology Department, 310 Lewis Hall, Montana State University, Bozeman, MT 59717, USA*

Summary Conventional wisdom holds that the ratio of leaf area to sapwood area (L/S) should decline during height (H) growth to maintain hydraulic homeostasis and prevent stomatal conductance (g_s) from declining. We contend that L/S should increase with H based on a numerical simulation, a mathematical analysis and a conceptual argument: (1) numerical simulation—a tree growth model, DESPOT (Deducing Emergent Structure and Physiology Of Trees), in which carbon (C) allocation is regulated to maximize C gain, predicts L/S should increase during most of H growth; (2) mathematical analysis—the formal criterion for optimal C allocation, applied to a simplified analytical model of whole tree carbon–water balance, predicts L/S should increase with H if leaf-level gas exchange parameters including g_s are conserved; and (3) conceptual argument—photosynthesis is limited by several substitutable resources (chiefly nitrogen (N), water and light) and H growth increases the C cost of water transport but not necessarily of N and light capture, so if the goal is to maximize C gain or growth, allocation should shift in favor of increasing photosynthetic capacity and irradiance, rather than sustaining g_s. Although many data are consistent with the prediction that L/S should decline with H, many others are not, and we discuss possible reasons for these discrepancies.

Keywords: carbon allocation, hydraulic homeostasis, optimization, resource substitution.

Introduction

Tree growth requires photosynthetic carbon (C) gain, which is limited by stomatal conductance (g_s). For a given leaf-to-air evaporative gradient (D), g_s is limited in turn by the tree's capacity to supply water to the canopy. Whitehead et al. (1984) combined an expression for xylem sap flow based on Darcy's Law with the Penman-Monteith equation for canopy transpiration to produce an identity showing how g_s and leaf water potential (Ψ_l) are linked to structural features such as the ratio of leaf area to sapwood area (L/S), axial flow path length (l) and xylem permeability (k_s). One expression of that identity is:

$$g_s l \frac{L}{S} \frac{1}{k_s} = \frac{(\Psi_s - \Psi_l - \rho g_{grav} h)}{D \eta V_w} \tag{1}$$

where Ψ_s is soil water potential, g_{grav} is gravitational acceleration, h is the vertical distance spanned by l and ρ, η and V_w are the density, dynamic viscosity and molar volume of water, respectively; units and definitions are given in Tables 1 and 2. Equation 1 shows that, to maintain hydraulic balance for any given Ψ_s and D, the increased path length and gravitational head concomitant with height (H) growth must be offset either by a reduction in g_s, L/S or Ψ_l, or by an increase in k_s.

Available data suggest compensation occurs in various subsets of these variables for different tree species and sites. Yoder et al. (1994) found reduced g_s in larger lodgepole pine trees, concurrent with a reduction in stand-level net primary productivity (NPP) that could not be attributed to increased respiration (Ryan and Waring 1992). In light of those data, Ryan and Yoder (1997) proposed the hydraulic limitation hypothesis, which holds that reduced g_s causes NPP to decline in aging forest stands. Some other authors have also found lower g_s in larger trees (McDowell et al. 2002b, Phillips et al. 2003, Delzon et al. 2004), although McDowell et al. (2002b) reported similar g_s in three H classes of Douglas-fir during summer drought and Barnard and Ryan (2003) found no effect of H on g_s during part of the growing season in *Eucalyptus saligna* Sm.

Hydraulic limitation of g_s by increasing path length could be prevented by structural compensation, particularly a reduction in L/S (e.g., Whitehead and Jarvis 1981, Whitehead et al. 1984, Becker et al. 2000). Many studies have found a decline in L/S with H (Mencuccini and Grace 1996, Ryan et al. 2000, Schafer et al. 2000, McDowell et al. 2002a, Delzon et al. 2004), but many data show the opposite trend (Dean and Long 1986, Long and Smith 1988, Gerrish 1990, Dunn and Connor 1993, Vertessy et al. 1995, Watson et al. 1999, Callaway et al.

Table 1. Parameters in DESPOT referred to in this paper. Most of the following parameter values were estimated for lodgepole pine (*Pinus contorta* Dougl. ex. Loud.), as described in the accompanying paper (Buckley and Roberts 2006). Source notations are as follows: (1) Ryan and Waring (1992); (2) Murty et al. (1996); (3) Whitehead et al. (1984); (4) observations by the authors; (5) Ryan (1991); (6) Ryan (1989); (7) Yoder et al. (1994); (*) see details under *Parameter estimation* in Appendix of Buckley and Roberts 2006; and (†) assumption. Abbreviations: C = carbon; and N = nitrogen.

Parameter	Symbol	Value	Units	Source
Leaf-to-air water vapor mole fraction gradient	D	0.015	mol H_2O mol^{-1}	†
Construction respiration fraction	f_c	0.22	–	1
Sapwood permeability	k_s	2.05×10^{-12}	m^2	3
Leaf and fine root maintenance respiration per unit N	v	0.041	mol C $year^{-1}$ $mmol^{-1}$N	5
Nitrogen content of sapwood	n_{sw}	1.2	mmol N mol^{-1}C	2
Wood C density	ρ_{cw}	1.4×10^4	mol C m^{-3}	6
Leaf area per unit C	SLA	0.091	m^2 mol^{-1}C	2
Median leaf lifespan	τ_l	8.3	Year	2
Median sapwood lifespan	τ_{sw}	14	Year	4
Windthrow risk parameter for stem breakage	w_b	1.15×10^5	–	*
Leaf water potential	Ψ_l	−1.5	MPa	7
Soil water potential	Ψ_s	−0.5	MPa	7

2000, Köstner et al. 2002, two of nine spp. in McDowell et al. 2002*a*, Mokany et al. 2003, Phillips et al. 2003). There is also evidence of compensation in k_s and Ψ_l: new conduit diameters are often larger in taller trees (e.g., Pothier et al. 1989, Maherali et al. 1997, Mencuccini et al. 1997, Spicer and Gartner 2001, Mokany et al. 2003) and both McDowell et al.

(2002*b*) and Barnard et al. (2003) found reductions in Ψ_l with H greater than needed to offset gravitational head. On the other hand, Delzon et al. (2004) reported a decrease in the driving gradient for water flow in taller maritime pine trees, and McDowell et al. (2002*b*) found smaller new conduit diameters in taller Douglas-fir.

Table 2. Variables in DESPOT referred to in this paper. Subscripts for allocation fractions, carbon pools and marginal gains are: l = leaves; r = fine roots; sw = sapwood; hw = heartwood; w = total wood; t = total carbon (sum of all pools); d = radial sw allocation; h = aboveground axial sw allocation; and z = belowground axial sw allocation. Abbreviations: C = carbon; and N = nitrogen.

Variable	Symbol	Units
Allocation fractions (x = l,r,d,h,z)	a_x	–
Leaf net CO_2 assimilation rate	A	µmol C m^{-2} s^{-1}
Single tree net primary production	A_n	mol C $year^{-1}$
Single tree gross primary production	A_t	mol C $year^{-1}$
Intercellular CO_2 mole fraction	c_i	µmol CO_2 mol^{-1}
Carbon pools (x = l,r,sw,hw,w,t)	C_x	mol C
Leaf level transpiration rate	E	mmol H_2O m^{-2} s^{-1}
Whole tree transpiration rate	E_t	mol H_2O s^{-1}
Stomatal conductance to H_2O	g_s	mol m^{-2} s^{-1}
Vertical span of axial flow pathlength	H	M
Tree height	H	M
Whole tree light capture	I_t	µmol s^{-1}
Leaf-specific hydraulic conductance	K_L	mmol H_2O m^{-2} s^{-1} MPa^{-1}
Axial flow pathlength	l	M
Leaf area, projected leaf area	L, L_p	m^2
Stand-level leaf area index	LAI	m^2 m^{-2}
Stand-level net primary productivity	NPP	kg C m^{-2} $year^{-1}$
Canopy photosynthetic nitrogen content	N_t	mmol N
Probability of stem breakage	p_b	–
Canopy laminar resistance	r_l	(mol $H_2O)^{-1}$ s MPa
Soil-xylem hydraulic resistance	r_s	(mol $H_2O)^{-1}$ s MPa
Axial (xylem) hydraulic resistance	r_x	(mol $H_2O)^{-1}$ s MPa
Sapwood area	S	m^2
Maximum RuBP carboxylation velocity	V_m	µmol CO_2 m^{-2} s^{-1}
Marginal gain from investment in C_x (x = l,r,sw,hw,w,t)	Ω_x	$year^{-1}$

In recent years, there has been a broad and intensive effort to characterize trends in structural adaptation of hydraulic function in the context of alternative hypotheses. This effort has delivered disparate results lacking a coherent explanation, perhaps because none of the alternatives (changes in g_s, L/S, k_s or Ψ_l) clearly represents the hypothesis that tree growth is adaptive with respect to a well-defined goal. Rather, these alternatives are just conveniently separable components of the physical constraints on steady-state water flow expressed by Equation 1. In other words, the physical theory delineates alternatives but does not suggest which is more likely, and experiments have not shown that any single pattern of hydraulic adjustment predominates in nature.

Much work to date has discussed the adaptive adjustment of hydraulic structure and function in terms of hydraulic balance alone (e.g., Whitehead et al. 1984, Magnani et al. 2000, Williams et al. 2001, Delzon et al. 2004). Although this seems reasonable, the variables in question are linked in a complex web of interacting costs and benefits that define the economic landscape on which whole-tree C allocation is adaptively regulated in growing trees. By focusing strictly on hydraulics, one risks omitting features that may influence that landscape in powerful and perhaps counterintuitive ways, such as photosynthetic resource substitution and light competition (e.g., Köstner et al. 2002).

The objective of this study was to offer a different theoretical perspective on hydraulic adjustment based on an explicit optimization hypothesis, in the hope of refocusing experimental efforts on the goals and constraints that shape adaptive tree growth. We ask what trajectories of L/S, g_s and H are predicted from the generic hypothesis that tree structure and function are regulated to maximize C gain, subject to known constraints of physics and biochemistry. To do this, we analyzed the behavior of a tree growth model called DESPOT (Deducing Emergent Structure and Physiology Of Trees), which is presented in the accompanying paper (Buckley and Roberts 2006). Carbon allocation in DESPOT is continuously regulated to maximize C gain, which is simulated by process models for photosynthesis and for the capture and delivery of substitutable photosynthetic resources.

The model

This section briefly describes the DESPOT model. A full description of the model is given in the accompanying paper (Buckley and Roberts 2006). Further details and mathematical derivations specific to this paper are presented in the Appendix. Parameters and variables are given in Tables 1 and 2; most parameter values were estimated to mimic the lodgepole pine chronosequence (*Pinus contorta* Dougl. ex. Loud.) studied by Ryan and Waring (1992), Yoder et al. (1994) and Murty et al. (1996).

Carbon is allocated among fine roots, leaves and sapwood based on five allocation fractions (three for sapwood, controlling growth in stem diameter, H and root depth independently). In each time step, a numerical algorithm identifies the set of allocation fractions that maximizes single-tree net structural C gain, or equivalently, either relative or absolute growth rate, in the next time-step. Gross C gain is simulated with a big-leaf version of the photosynthesis model of Farquhar et al. (1980), in which CO_2-saturated assimilation rate depends on leaf nitrogen (N) and incident irradiance, and CO_2 supply depends on g_s, and thus on transpiration rate and evaporative gradient. Light capture is modeled by Beer's Law. Canopy N content is simulated dynamically based on uptake by fine roots and losses due to leaf senescence, accounting for N demands of new fine roots and sapwood. Canopy transpiration is proportional to the soil–leaf pressure gradient and inversely proportional to the serial sum of three resistances: from the soil to the root xylem, through the root and stem xylem and through the leaf itself. Leaf water potential is either assumed constant or allowed to decline to offset gravitational head; in the latter case, embolism-related costs of declining Ψ_l are evaluated in additional simulations.

Maintenance respiration is proportional to tissue N content (with constant N/C ratios for fine roots and wood, but not for leaves), and construction respiration is a fixed fraction of net C gain. Senescence and heartwood conversion are simulated by tracking each new tissue increment individually and progressively reducing its surviving fraction according to a tissue-specific Weibull lifespan distribution. The constraints due to windthrow risk on diameter versus H and below- versus aboveground biomass relationships are treated probabilistically: candidate allocation vectors are penalized in proportion to the likelihood that they will produce mechanically untenable geometries, in order to make those allocation vectors appear unprofitable to the optimization algorithm. The available ground area per tree and aspects of canopy geometry needed to estimate the benefit of H growth are simulated by assuming the stand is uniform and that it self-thins according to the –3/2 power law.

Results

The accompanying paper (Buckley and Roberts 2006) describes the DESPOT model and its general behavior and compares some of its predictions with data from a lodgepole pine (*Pinus contorta*) chronosequence studied by Ryan and Waring (1992). Here, we present and discuss DESPOT's behavior in the context of adjustment to the hydraulic burdens created by H growth.

Structural-functional adjustment during height growth

Based on the standard parameter values given in Table 1 and assuming constant Ψ_l and k_s, DESPOT predicts that L/S should decrease briefly during early H growth, but then increase progressively until H growth tapers off (Figure 1a). Conversely, the model predicts that g_s (Figure 1b) and leaf-specific hydraulic conductance (K_L, Figure 1b) should both decline with H during most of H growth. DESPOT also predicts that leaf-level irradiance (I; Figure 2a) should decline but photosynthetic capacity (V_m; Figure 2a) should remain rough-
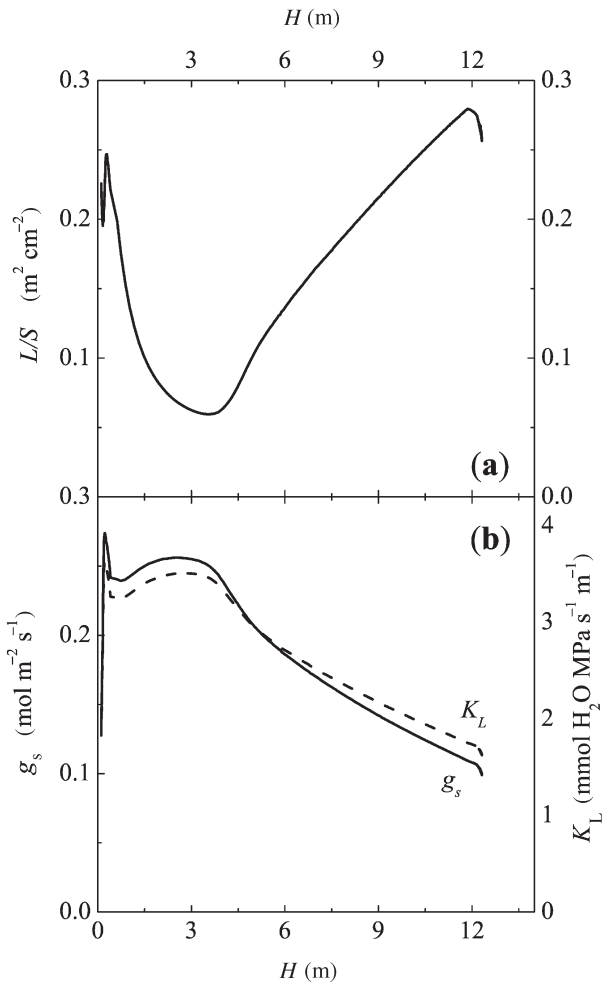
Figure 1. Relationships predicted by DESPOT between tree height (H) and (a) leaf area/sapwood area ratio (L/S) and (b) stomatal conductance (g_s) and leaf-specific hydraulic conductance (K_L). These simulations assumed constant leaf water potential and sapwood permeability.
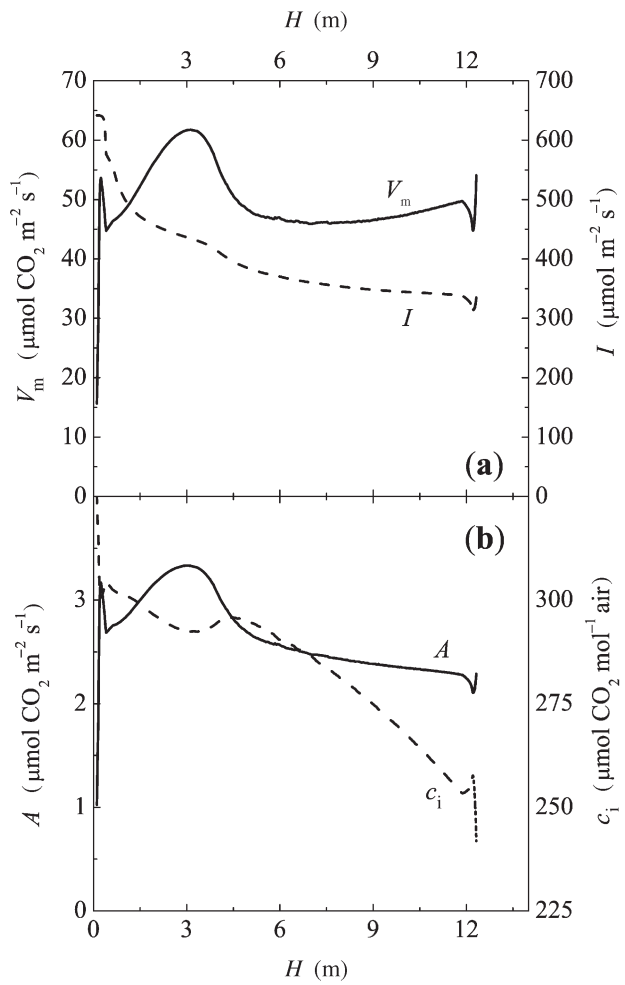
Figure 2. Relationships predicted by DESPOT between tree height (H) and leaf-level photosynthetic variables: (a) photosynthetic capacity (V_m) and irradiance (I) and (b) net CO_2 assimilation rate (A) and intercellular CO_2 mole fraction (c_i). These simulations assumed constant leaf water potential and sapwood permeability.

ly steady during most of H growth.

As a result of these shifts in leaf-level photosynthetic resource investment, both leaf-level net CO_2 assimilation rate (A; Figure 2b) and intercellular CO_2 mole fraction (c_i; Figure 2b) decline with H. However, a concurrent increase in leaf area index (LAI; Figure 3a) mostly offsets the decline in A, preventing net C gain per unit ground area (NPP; Figure 3a) from declining substantially. This increase in LAI also creates a different pattern of change in photosynthetic resource use variables expressed on a ground area basis (Figure 3b): water use declines for most of H growth, but this is offset by concurrent increases in both N and light use, in contrast to the trends predicted for the leaf-level variables.

Alternative assumptions regarding hydraulic homeostasis

We performed additional simulations based on two alternative assumptions about hydraulic homeostasis: (a) permeability of new sapwood (k_s) increases by 1×10^{-12} m^2 per 10 m of axial

path length under isohydric conditions (this doubles k_s from its nominal value of 2×10^{-12} m^2 when path length is 20 m), or (b) Ψ_l is allowed to decline enough to offset gravitational head (so that $\Psi_l + \rho g h$, not Ψ_l itself, is constant over time). In case (b), the possible increase in embolism frequency at reduced Ψ_l was simulated in two ways: (1) by reducing the annual period of active photosynthesis with h, such that it declines by half at $h = 10.2$ m (which was the value of h at maturity in standard simulations); or (2) by simulating more frequent unrecoverable embolism by increasing the sapwood failure rate (such that it doubled at $h = 10.2$ m). Similar qualitative trends were predicted between H and L/S, g_s and c_i under all of these scenarios (Figure 4).

Simulations with altered algorithm for optimizing allocation

To determine how DESPOT's predictions would be affected by imprecision in C allocation, we performed an additional simulation using modified parameter values for the model's
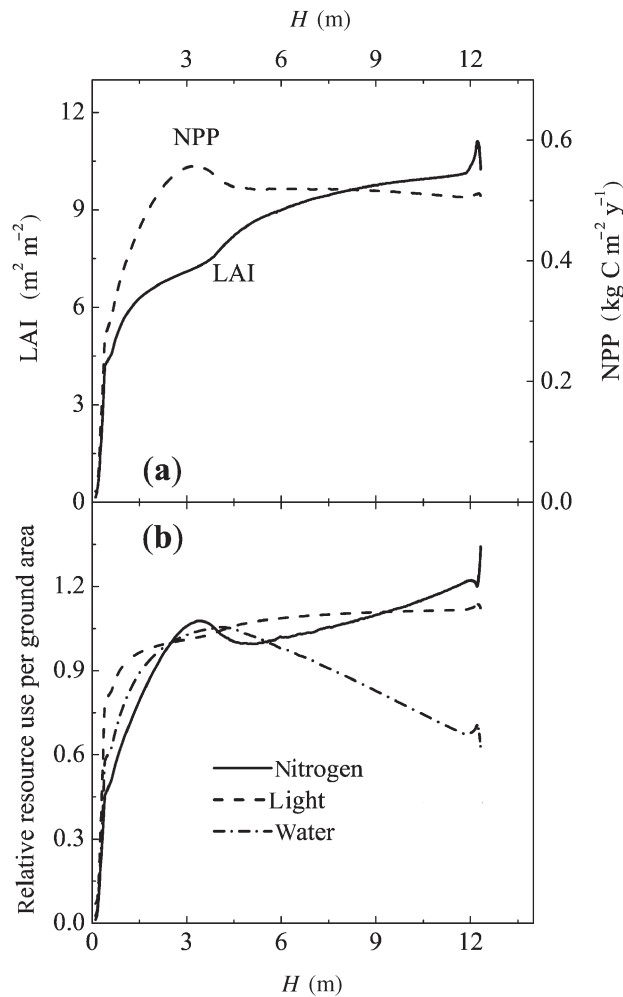
Figure 3. Relationships predicted by DESPOT between tree height (H) and several variables expressed on a ground area basis: (a) leaf area index (LAI) and net primary productivity (NPP) and (b) transpiration rate, canopy nitrogen content and light capture expressed relative to their values at $H = 2.5$ m (the point at which stomatal conductance (g_s) began to decline continuously; cf. Figure 1b). These simulations assumed constant leaf water potential and sapwood permeability.

Figure 4. Relationships predicted by DESPOT between tree height (H) and (a) leaf area/sapwood area ratio (L/S) (b) stomatal conductance (g_s) and (c) intercellular CO_2 mole fraction (c_i) under alternative assumptions about hydraulic homeostasis: constant bulk leaf water potential (Ψ_l) and sapwood (sw) permeability (k_s) (solid lines), constant Ψ_l and increasing k_s with path length ("$+ k_s$"), constant pressure gradient and reduced period of active gas exchange due to increased cavitation repair ("$-$ time"), or constant pressure gradient and increased sapwood failure rate to represent greater frequency of unrecoverable embolism ("$+$ sw fail rate").

numerical solution procedure, a hybrid genetic algorithm/Monte Carlo method described in the accompanying paper (Buckley and Roberts 2006). Briefly, the method starts in each timestep with nm randomly chosen allocation vectors, finds the m best-performing vectors, chooses nm new vectors by randomly "mutating" each component of these m vectors n times in a range of $(1 \pm B)$ times their original values, and then repeats the cycle until all n vectors perform similarly, within some tolerance.

We reduced the likelihood of finding the true global optimum by seeding each solution cycle with fewer randomized guesses (reducing n from 500 to 50) and by reducing the degree of mutation (reducing B from 0.5 to 0.1). We also performed an additional simulation in which the optimization algorithm itself was suspended at 60 years (shortly before the
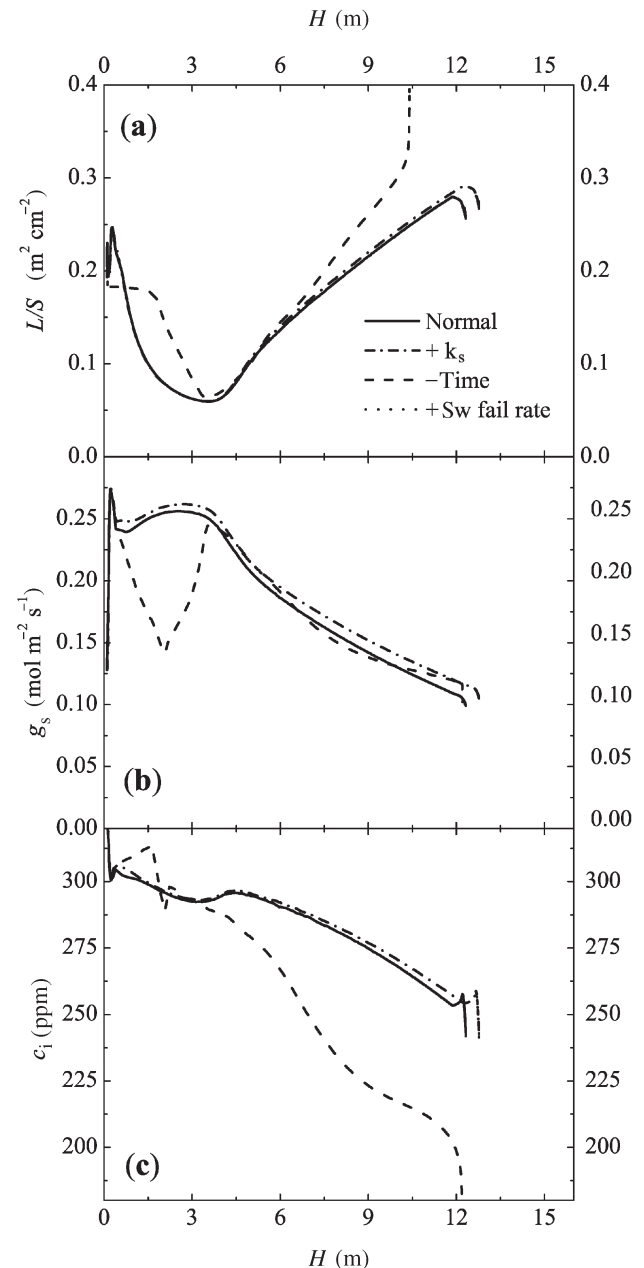
cessation of H growth), and the average values of each allocation fraction over the preceding 100 time steps (2 years) were used for the remainder of the simulation. In both of these simulations, NPP declined over time and H growth continued indefinitely (Figure 5).

Discussion

Some of DESPOT's predictions about structural and functional adjustment during H growth are broadly consistent with published observations. Several studies have reported reduced A and g_s in taller trees during at least part of the growing season (Yoder et al. 1994, McDowell et al. 2002b, Barnard and Ryan 2003, Delzon et al. 2004, Koch et al. 2004), and the prediction of reduced g_s parallels the hydraulic limitation hypothesis (Ryan and Yoder 1997). Declining K_L with H also appears to
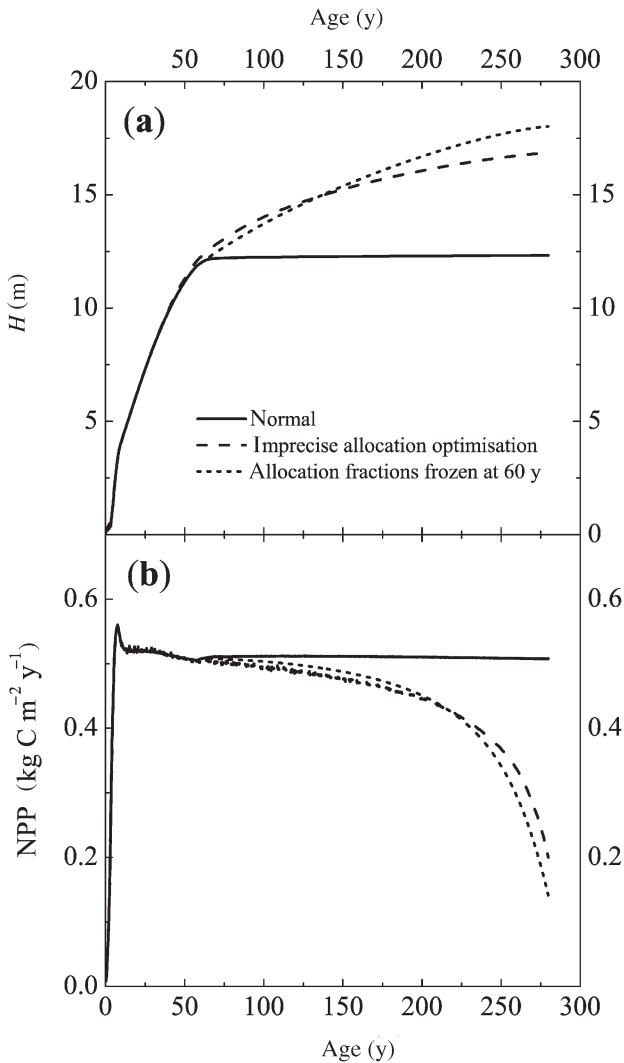

Figure 5. Trajectories of tree height (H) and net primary productivity (NPP) predicted by DESPOT under normal simulation parameters (solid lines); when parameters controlling the precision of the model's numerical optimization algorithm were altered to simulate imperfection in the mechanisms that control carbon allocation (long-dash lines); or when allocation fractions were permanently frozen at 60 years, rather than being continuously optimized for the remainder of the simulation (short-dash lines). Details of the numerical method are given in the accompanying paper (Buckley and Roberts 2006); simulations indicated by solid and long-dashed lines used 500 and 50 initial Monte Carlo seeding guesses, respectively, and mutated each solution cycle's best guesses by ± 50% or 10%, respectively, to seed the next cycle.

be a nearly universal phenomenon (Saliendra et al. 1995, Mencuccini and Grace 1996, McDowell et al. 2002b, Barnard and Ryan 2003, Mokany et al. 2003, Delzon et al. 2004). Many authors have found H-related reductions in c_i or in C isotope discrimination, a proxy for c_i (Yoder et al. 1994, McDowell et al. 2002b, Barnard and Ryan 2003, Delzon et al. 2004, Koch et al. 2004), as predicted by DESPOT. However, although Barnard and Ryan (2003) found less discrimination (indicating lower c_i) in upper leaves than in lower leaves of age-matched trees, they found the opposite trend among trees of different heights.

Less consistent is the evidence bearing on DESPOT's prediction that leaf-level N and photosynthetic capacity remain roughly steady during H growth. Some authors have reported little or no change in these variables (Barnard and Ryan 2003, Koch et al. 2004), whereas others have found declines (Grulke and Miller 1994, Schoettle 1994, McDowell et al. 2002b).

The most surprising of DESPOT's predictions, however, is that L/S should increase with H during most of H growth. This is consistent with some data (Dean and Long 1986, Long and Smith 1988, Gerrish 1990, Vertessy et al. 1995, Watson et al. 1999, Callaway et al. 2000, Köstner et al. 2002, McDowell et al. 2002a, Mokany et al. 2003, Phillips et al. 2003), but contradicts many other observations, including seven of nine species evaluated in a recent meta-analysis by McDowell et al. (2002a). The explanation for the more common observation that L/S declines with H is based on the premise that the increased hydraulic burdens caused by H growth require greater S to sustain a water flow to a given L. To unravel this paradox, it is necessary to examine closely some common ideas about water relations and C gain.

The first point, which was noted by Köstner et al. (2002), is that Equation 1 shows L/S must decrease with H to sustain g_s and Ψ_l, not C gain. Structural compensation to sustain g_s is not necessarily an optimal tactic for C allocation. Although it may seem reasonable to suppose that C gain will decline if g_s declines, whole-tree C gain can be sustained despite declining g_s if the reduction in g_s is matched by appropriate increases in L (as noted by McDowell et al. 2002a) or in leaf-level photosynthetic capacity or irradiance. This is because a given rate of CO_2 fixation can be achieved with nearly any combination of three resources—N, light and transpirable water. Resource substitution can decouple C gain from hydraulic balance, allowing g_s to decline with H without reducing C gain. Empirical evidence demonstrating the possibility of photosynthetic resource substitution is abundant. A classic study by Field et al. (1983) found a distinct tradeoff between water- and N-use efficiency in California chapparal species and Schulze et al. (1998) and Miller et al. (2001) found an inverse relationship between leaf N content and rainfall along a precipitation gradient in Australia. Theoretical support was also provided by Smith and Huston (1989), who hypothesized a similar tradeoff between light and water and by Hilbert and Reynolds (1991), who predicted that optimal leaf N content should be lower at high CO_2 concentrations. The latter authors also remarked that "a whole plant perspective is necessary in order to understand the adaptive significance of plant traits like photosynthetic ca-

pacity"—a prescient comment in light of the current controversy over the nature of physiological adjustment during H growth.

Photosynthetic resource substitution makes it unnecessary for L/S to decline with H for g_s to be sustained, but it does not explain why L/S should increase with H. To explain this, it helps to focus more directly on how resource substitution is achieved in the DESPOT model. Height growth in DESPOT is accompanied by increasing LAI (Figure 3a), which counteracts the decline in leaf-level C gain (Figure 2b), preventing NPP from declining substantially (Figure 3a). It also "spreads" the total photosynthetic resource supplies over a progressively larger area, which obscures the occurrence of whole-tree resource substitution. When total photosynthetic resource use is expressed on a ground area basis to account for changes in single-tree L and stand density, water use declines by 31% during H growth, but total N and light use both increase by 13–14% (Figure 3b). In other words, the increase in L permits a decline in water use by capturing more light, and thus increasing CO_2 demand. This contradicts the perception that greater L implies greater water demand, which is correct only if g_s is constrained to invariance. (The correlation between LAI and site water balance reported by Grier and Waring (1977) and Waring et al. (1978) is emergent, but not necessarily causal: L determines the intensive (area-based) transpiration rate and g_s ($\approx E/D = E_t/LD$) that can occur in steady-state with a given total rate of water flow to the canopy, but it does not independently control whole-tree transpiration rate.)

To summarize, DESPOT substitutes light and N for water during H growth, and one effect of the changes in allocation required to achieve this is that L/S increases. But why does this maximize C gain and why is it not preferable to shore up water supply instead? Formal optimality theory can provide some insight here. It predicts that a finite C supply earns the greatest profit—i.e., it is optimally distributed—if a little extra C would earn the same profit regardless of where it was invested (with the caveat that C earns diminishing returns in each investment site). In economic terms, the marginal gain from C investment should be invariant among investment sites (see Equation A6). It is therefore useful to ask how the marginal gains for C investment in S and L vary with H in a growing tree. The marginal gain for radial sapwood C production, Ω_{sd} (derived in the Appendix) is:

$$
\left(\frac{\partial A_n}{\partial C_{sw}}\right)_{H,Z} = \left(\frac{\dfrac{L}{S}\left(\dfrac{A/(1+g_s/g_m)}{l\eta V_w + k_s S(r_s + r_1)}\right) \times}{\dfrac{\eta V_w}{\rho_{cw}} - vn_{sw}} \right)(1 - f_c) \quad (2)
$$

where g_m, the slope of the A versus c_i curve, is determined by photosynthetic capacity, irradiance and g_s; r_s and r_1 are soil–root and laminar resistances; ρ_{cw} is wood C density; vn_{sw} is respiration per unit sapwood C; and f_c is the construction respiration fraction. Equation 2 shows that the return on S production declines with path length but increases with L/S if leaf-level

photosynthetic variables are constant (A, g_s, V_m and I, and hence g_m). To identify the optimal trend between L/S and path length, we use the formal condition of optimality: equality of marginal gains, or $\Omega_{sd} = W_1$, where W_1 is the marginal gain from C investment in leaves. If leaf laminar resistance can be ignored to a first approximation, W_1 does not depend explicitly on either path length or L/S (as shown in the Appendix), so W_1 can be treated as an independent parameter in Equation 2. This allows the condition $\Omega_{sd} = W_1$ to be solved for L/S as a function of path length:

$$
\frac{L}{S} = (l\eta V_w + k_s S r_s)\left(\frac{\Omega_1}{1 - f_c} + vn_{sw}\right) \times
$$
$$
\left(\frac{1 + g_s/g_m}{A}\right)\frac{\rho_{cw}}{\eta V_w} \quad (3)
$$

Thus, all else being equal, L/S should increase as path length increases, if the goal is to maximize net C gain or growth.

All else is probably not equal

Magnani et al. (2000) reached the opposite conclusion by equating the sensitivities of total hydraulic resistance to C investment in fine roots or sapwood and solving for various allometries. However, that analysis treated hydraulic homeostasis as the goal, so it excluded any non-hydraulic effects of C allocation, thereby precluding resource substitution at the outset. Similar criticisms must also be leveled against Equation 3, which was obtained only by arbitrarily ignoring some costs and benefits. For example, Equation 2 does not account for the mitigation of windthrow risk by radial growth. More generally, leaf laminar resistance probably cannot be ignored, and it, along with many other factors that affect Ω_w and Ω_1, may vary during the course of tree growth. We do not believe that the human mind can simultaneously assess more than a few such factors—the caveat of "all else being equal" is an illusory crutch and a logical trap. The analytical simplicity that it confers cannot be retained without being tested, but it cannot be tested without being discarded by resorting to numerical solution. It is meaningful only insofar as we choose to believe its untested assumptions.

To illustrate this point, we examine the model's prediction that L/S should briefly decline with H during the early part of H growth (Figure 1a), which contradicts Equation 3. The reason apparently involves windthrow risk dynamics, which were omitted from the derivation of Equation 3 for the sake of analytical solution. A rapid increase in the probability of stem breakage (p_b) occurs in the initial rapid phase of H growth, when stem elongation increases the turning moment that can be applied to the base of the trunk by the force of wind on the canopy (Equations A22 and A23 in Buckley and Roberts 2006). This increases the benefit of radial trunk growth, and hence of S production, as perceived by the model's optimization algorithm (which maximizes the product of net C gain and windthrow risk).

To evaluate the consistency of this explanation, we performed several additional simulations. In two of these, we increased the parameter w_b by two or four times its usual value (w_b controls the critical windspeed for wind-induced trunk breakage, and thus determines how much radial growth is needed to support a given amount of H growth). In each case, S and L followed a fairly conserved long-term trend, but S increased transiently above this trend at the same time that p_b increased during the rapid H growth phase (Figure 6a). However, the size of the transient increase in S was smaller for larger w_b (Figure 6b), suggesting that the rise in S represents a response to windthrow risk rather than to the hydraulic burden of H growth. To further test this idea, we performed another simulation in which we modified the DESPOT program to artificially increase sapwood permeability (k_s) by a factor of 10 whenever $p_b > 0$. This would greatly reduce the hydraulic incentive to increase S, enabling any spike in S to be attributed more confidently to the mechanical incentive. In this simulation, a spike in S occurred that was similar in magnitude to the spike predicted under normal conditions, and which also coincided with the spike in p_b caused by rapid H growth (Figure 6b). This strongly suggests that the simulated decline in L/S during early H growth is caused by mechanical, not hydraulic factors.

Why does L/S decrease with height in some trees?

Many studies have found L/S decreases with H, which our analysis suggests should generally be counterproductive. Below, we discuss five possible reasons for these discrepancies: (1) the increased C cost of water transport due to H growth is exceeded by concomitant increases in the costs of N or light capture, (2) L/S may not simply reflect L and S production rates, because the delayed and variable effects of senescence decouple production rates from pool sizes, (3) some critical aspect of DESPOT's process structure is incorrect, (4) the optimal allocation patterns predicted by DESPOT cannot be achieved in practice, because of genetic or physiological constraints or random environmental disturbance, or (5) C allocation is driven by a goal other than continuous maximization of C gain or growth.

(1) Increased cost of nitrogen or light with H growth This could result from progressive depletion of soil N in early growth. Our model does not explicitly simulate soil N cycling, so it cannot evaluate this possibility. Increased non-hydraulic costs could also result from a tragedy of the commons caused by aggressive competition, similar to that predicted by Schieving and Poorter (1999) for two co-occurring canopy species with different specific leaf areas. In DESPOT, overlap with adjacent canopies would create laterally patchy LAI, reducing total light capture at a given stand LAI. Similar effects could also result from localized depletion of soil resources as a result of overlap of extraction zones.

(2) Sapwood lasts much longer than leaves Whether L/S rises or falls if sapwood production declines relative to leaf production depends on sapwood and leaf longevities, and on their
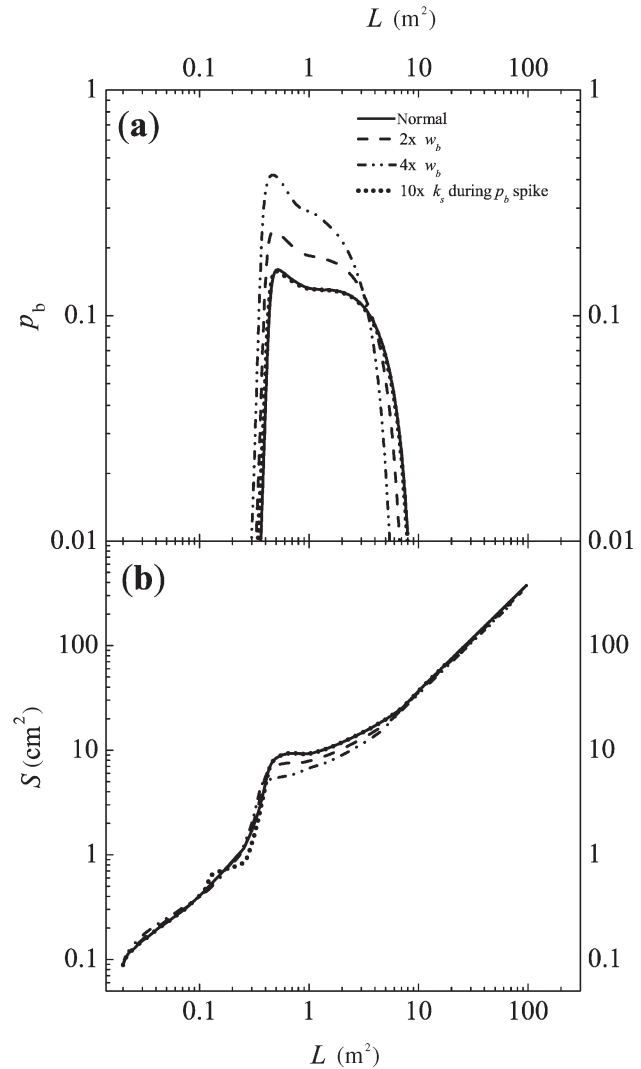

Figure 6. Trajectories of (a) the probability of windthrow due to stem breakage, p_b, and (b) sapwood area, S, both plotted against leaf area, L, on a logarithmic axis to enable dynamics across a wide range of scales to be visualised more clearly. The solid line represents trajectories under "standard" conditions; the lines labeled "2x w_b" and "4x w_b" are trajectories from simulations in which the parameter w_b was set at two or four times its normal value, respectively; the lines labelled "10 x k_s during p_b spike" are from a simulation in which sapwood permeability (k_s) was artificially increased tenfold whenever $p_b > 0$. See the text for details.

prior history of production. To a first approximation, senescence rates are proportional to pool sizes, in which case:

$$\frac{d}{dt}\left(\frac{L}{S}\right) \propto A_n\left(\frac{a_1}{C_1} - \frac{a_d}{C_{sw}}\right) - \left(\frac{\tau_{sw} - \tau_1}{\tau_{sw}\tau_1}\right) \qquad (4)$$

where τ_1 and τ_{sw} are leaf and sapwood longevity, respectively, and a_1 and a_d are fractions of C allocated to leaf and radial sapwood production, respectively (Equation 4 is derived in the Appendix). This shows that, if sapwood lasts longer than

leaves ($\tau_{sw} > \tau_l$), L/S can decline over time even if radial sapwood production ceases entirely ($a_d \rightarrow 0$).

(3) DESPOT is critically flawed or incomplete   The purpose of DESPOT is to see what aspects of tree growth can be predicted from physiological constraints and the hypothesis of profit-maximizing C allocation. Therefore, by design, the model excludes ecosystem processes like resource competition and soil N cycling (mentioned above), and community processes like demographic stratification and succession. Although the significance of community dynamics for L/S are not intuitively obvious, it is clear that early- and late-successional species experience different patterns of change in resource availability during H growth. Callaway et al. (2000) found that stand-level trends in productivity and L/S were confounded by succession from whitebark pine, a shade-intolerant species, to subalpine fir, a shade-tolerant species. Specifically, the L/S ratio (inferred from biomass allometries) declined over time for whitebark pine, but varied little throughout succession for subalpine fir.

Another open question about DESPOT's process structure is how best to model hydraulic homeostasis. It seems fairly well established that g_s adjusts on long time scales to keep daily minimum water potential above a cavitation threshold (e.g., Sperry 2000), but it is less clear how that threshold, or the safety margin maintained by stomata, varies over months and years, as trees grow in H. DESPOT assumes isohydric behavior by default. The model also assumes that permeability of new sapwood is constant throughout growth, whereas k_s has often been found to increase with H (e.g., Maherali et al. 1997, Mencuccini et al. 1997, Spicer and Gartner 2001). However, we relaxed both of these assumptions in additional simulations and found that DESPOT still predicted an increase in L/S with H (Figure 4a).

(4) Optimal allocation is infeasible   Goal-directed models presume the existence of processes that can achieve the postulated goals. In reality, however, natural selection can isolate optima only from the set of alternatives generated by mutation and recombination, so if extant processes are optimal at all, they are so only in the unknowable context of a taxon's evolutionary history. To see how DESPOT's predictions would differ if allocation were suboptimal, we performed two additional simulations. In one, we reduced the precision of the optimization algorithm; in the other, allocation fractions were "frozen" at 60 years, just as H growth was tapering off. In both cases, H growth continued indefinitely and productivity declined (Figure 5). This contrasts with the standard DESPOT simulations but is consistent with the premise that imprecise allocation can significantly influence growth trajectories. However, L/S still increased with H during most of H growth in those simulations (not shown). That such a large change in the trajectory of NPP was induced by fixing allocation fractions suggests that when models are used to evaluate the effects of various physiological and ecological constraints on productivity, the method of modeling allocation may itself deserve consideration as an additional constraint.

DESPOT implicitly assumes that trees are sufficiently plastic to achieve the calculated optimal course of resource substitution, but some evidence suggests that some species have severely limited allocation plasticity. For example, Miller (2002) evaluated trends in leaf N content and C isotope discrimination along a rainfall gradient in the Northern Territory, Australia, using formal economic theory to quantify the extent to which *Eucalyptus* species substituted N for water in drier environments. He found pronounced resource substitution in general, both within and among species. However, he found that species differed in the degree to which they could shift allocation to match theoretically optimal patterns of N and water use.

(5) The goal is something other than maximizing growth
Another assumption common to goal-directed arguments in biology is that the observed patterns maximize reproductive success relative to alternatives. Many patterns of interest, however, do not affect reproductive success in a simple and calculable way. Therefore, many teleonomic plant models, including DESPOT, use C gain or growth as proxy goals. To the extent that reproductive success responds positively to carbohydrate supply or plant size, some measure of C gain or growth should accurately reflect how changes in C allocation patterns influence reproductive success. What is less clear is whether an appropriate measure of C gain can be defined locally in time, or if it must instead integrate behavior over a longer term.

Allocation patterns that are inefficient as measured by their effect on short-term growth may afford a reproductive advantage (Obeso 2002), so it is easy to imagine scenarios in which a shortsighted focus on immediate profit reduces long-term success. For example, an understory species may have a negligible chance of long-term success if it optimizes its structure and physiology for performance beneath an existing canopy. A better strategy may be to optimize for gap performance at the expense of growth before a gap opens. The efficacy of such a strategy cannot, however, be assessed from the state of the plant at any single moment, because its benefit is contingent on future events. A profit-based model like DESPOT would see only the costs of maintaining a gap-optimized canopy in the shade, such as the respiratory burden of high photosynthetic capacity. During this stage plants could store nitrogen which would enhance growth after the opening of a gap. However, a profit-driven model cannot predict the benefits of storage, because stored resources earn no immediate profits.

Two other features that may be difficult to explain by profit-driven allocation are H growth itself and the effect of H growth on productivity. As discussed in the accompanying paper (Buckley and Roberts 2006), DESPOT predicts determinate H growth and sustained NPP. King (1990) also predicted determinate H growth with an analytical cost/benefit model that maximized wood production. He noted, however, that this prediction contrasts with many data showing only a gradual cessation, if any, in H growth. Ryan and Waring (1992) similarly found continued H growth and declining productivity in a lodgepole pine chronosequence, and more generally, sustained NPP is the exception, not the rule (Ryan et al. 1997, but see

Callaway et al. 2000). This may indicate that H growth itself is more important for long-term success than is total growth or C gain potential, at least early in stand development.

We investigated this possibility by performing additional simulations in which the "goal function" for allocation was not A_n, but instead the quantity $H^b A_n^{1-b}$ (where $0 < b < 1$); this can be interpreted as an H-weighted growth rate, with $b/(1-b)$ a measure of the relative importance of H. For $0 \le b \le 0.3$, the same generic trends were predicted for most key variables, but final H increased and maximum productivity decreased linearly with b (Figure 7) (for $b \ge 0.4$, a stable solution could not be achieved). Similarly, the ratio of NPP/GPP declined significantly with H among mature trees with different parameter sets (Figure 8) in the Monte Carlo analysis presented in the accompanying paper (Buckley and Roberts 2006), and King's (1990) analysis predicted an evolutionarily stable H-growth strategy that reduced wood productivity relative to the theoretical maximum in the absence of competition. This is another example of the tragedy of the commons: H growth imposes unnecessary restrictions on water transport, so it can only reduce potential stand-level C gain.

Other modeling work supports the notion that short-term optimization may limit long-term success. Chen and Reynolds (1997) found that long-term ("global") and short-term ("local" or continuous) optimal allocation trajectories were identical during exponential growth under constant conditions, using a model that was simple enough to permit numerical calculation of long-term optima. However, when dramatic changes in environmental conditions were imposed, the global and local optima diverged. The global solution "knew" in advance about an imminent drought, so it preemptively shifted allocation in a manner that improved its post-drought success relative to the continuous optimum. Plants are known to possess mechanisms for "anticipatory" or feedforward behavior (for example, in the response of stomata to soil drought, e.g., Davies et al.

Figure 8. The ratio of NPP/GPP (net/gross primary productivity) as a function of tree height (H) at 200 years, for 48 different simulations among which all parameters in the model were randomly varied in a range of ± 25% of their nominal values. Each symbol represents a different simulation from the Monte Carlo parameter sensitivity analysis presented in the accompanying paper (Buckley and Roberts 2006).

1994), so it seems likely that C allocation can be influenced by factors other than the current state of the plant and its immediate environment.

Conclusion

We present predictions concerning hydraulic adjustment from an optimality-based tree growth model (DESPOT, described in the accompanying paper, Buckley and Roberts 2006) that accounts for photosynthetic resource substitution. DESPOT predicts that, if whole-tree C allocation is regulated to maximize C gain, then H growth should be accompanied by a decline in g_s and an increase in L/S. This contrasts with the conventional wisdom that L/S should decline with H, which is based on the assumption that the goal is to maintain constant leaf-level g_s. When g_s is instead allowed to vary, C allocation shifts from water transport toward the capture of N and light, which can substitute for water in photosynthetic C gain. As a result, H growth in DESPOT is also accompanied by a decrease in the intercellular CO_2 mole fraction (c_i) averaged over the canopy. Although some data are consistent with these predictions, many are not, which may suggest that tree C allocation cannot be explained by the goal of maximizing C gain continuously.
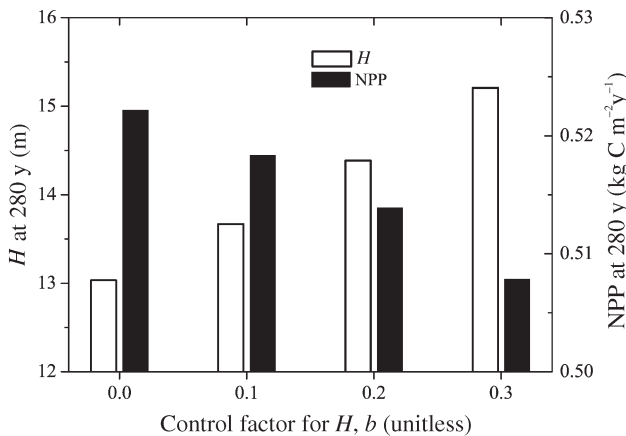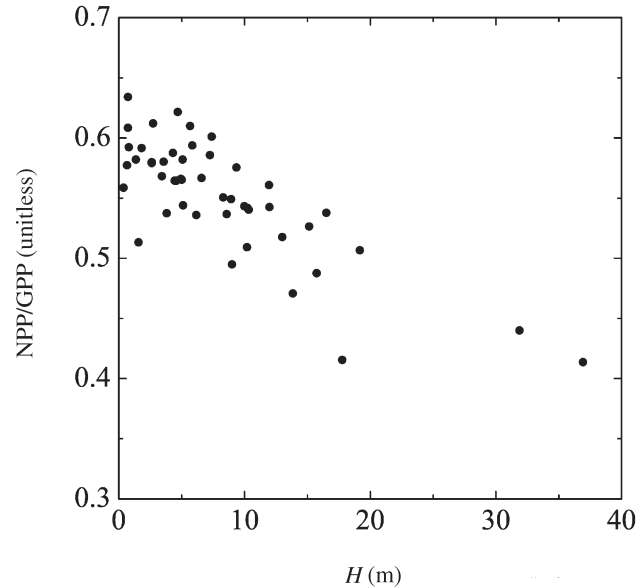

Figure 7. Tree height (H, open bars) and net primary productivity (NPP, closed bars) at 280 years in simulations wherein DESPOT was modified to maximize the product $H^b A_n^{1-b}$ for different values of the dimensionless parameter b (0.0, 0.1, 0.2 and 0.3, indicated on the horizontal axis), instead of simply maximizing A_n (where A_n is single-tree net carbon gain).

References

Barnard, H.R. and M.G. Ryan. 2003. A test of the hydraulic limitation hypothesis in fast-growing *Eucalyptus saligna*. Plant Cell Environ. 26:1235–1245.

Becker, P., F.C. Meinzer and S.D. Wullschleger. 2000. Hydraulic limitation of tree height: a critique. Funct. Ecol. 14:4–11.

Buckley, T.N. and D.W. Roberts. 2006. DESPOT, a process-based tree growth model that allocates carbon to maximize carbon gain. Tree Physiol. 26:129–144.

Buckley, T.N., J.M. Miller and G.D. Farquhar. 2002. The mathematics of linked optimization for nitrogen and water use in a canopy. Silva Fenn. 36:639–669.

Callaway, R.M., A. Sala and R.E. Keane. 2000. Succession may maintain high leaf area:sapwood ratios and productivity in old subalpine forests. Ecosystems 3:254–268.

Chen, J.-L. and J.F. Reynolds. 1997. A coordination model of whole-plant carbon allocation in relation to water stress. Ann. Bot. 80: 45–55.

Cowan, I.R. and G.D. Farquhar. 1977. Stomatal function in relation to leaf metabolism and environment. Symp. Soc. Exp. Biol. 31: 471–505.

Davies, W.J., F. Tardieu and C.L. Trejo. 1994. How do chemical signals work in plants that grow in drying soil? Plant Physiol. 104: 309–314.

Dean, T.J. and J.N. Long. 1986. Variation in sapwood area–leaf area relations within two stands of lodgepole pine. For. Sci. 32: 749–758.

Delzon, S., M. Sartore, R. Burlett, R. Dewar and D. Loustau. 2004. Hydraulic responses to height growth in maritime pine trees. Plant Cell Environ. 27:1077–1087.

Dunn, G.M. and D.J. Connor. 1993. An analysis of sap flow in mountain ash (*Eucalyptus regnans*) forests of different age. Tree Physiol. 13:321–336.

Farquhar, G.D. 1989. Models of integrated photosynthesis of cells and leaves. Phil. Trans. Roy. Soc. B. 323:357–367.

Farquhar, G.D., S. von Caemmerer and J.A. Berry. 1980. A biochemical model of photosynthetic CO_2 assimilation in leaves of C3 species. Planta 149:78–90.

Field, C. 1983. Allocating leaf nitrogen for the maximization of carbon gain: leaf age as a control on the allocation program. Oecologia 56:341–347.

Field, C., J. Merino and H.A. Mooney. 1983. Compromises between water-use efficiency and nitrogen-use efficiency in five species of California evergreens. Oecologia 60:384–389.

Gerrish, G. 1990. Relating carbon allocation patterns to tree senescence in *Metrosideros* forests. Ecology 71:1176–1184.

Grier, C.C. and R.H. Waring. 1977. Leaf area of mature northwestern coniferous forests: relation to site water balance. Ecology 58: 893–899.

Grulke, N.E. and P.R. Miller. 1994. Changes in gas exchange characteristics during the life span of giant sequoia: implications for response to current and future concentrations of atmospheric ozone. Tree Physiol. 14:659–668.

Hilbert, D.W. and J.F. Reynolds. 1991. A model allocating growth among leaf proteins, shoot structure, and root biomass to produce balanced activity. Ann. Bot. 68:417–425.

King, D.A. 1990. The adaptive significance of tree height. Am. Nat. 135:809–828.

Koch, G.W., S.C. Sillett, G.M. Jennings and S.D. Davis. 2004. The limits to tree height. Nature 42:851–854.

Köstner, B., E. Falge and J.D. Tenhunen. 2002. Age-related effects on leaf area/sapwood area relationships, canopy transpiration and carbon gain of Norway spruce stands (*Picea abies*) in the Fichtelgebirge, Germany. Tree Physiol. 22:567–574.

Long, J.N. and F.W. Smith. 1988. Leaf area–sapwood area relations of lodgepole pine as influenced by stand density and site index. Can. J. For. Res. 18:247–250.

Magnani, F., M. Mencuccini and J. Grace. 2000. Age-related decline in stand productivity: the role of structural acclimation under hydraulic constraints. Plant Cell Environ. 23:251–263.

Maherali, H., E.H. DeLucia and T.W. Sipe. 1997. Hydraulic adjustment of maple saplings to canopy gap formation. Oecologia 112: 472–480.

McDowell, N., H. Barnard, B.J. Bond et al. 2002*a*. The relationship between tree height and leaf area:sapwood area ratio. Oecologia 132:12–20.

McDowell, N.G., N. Phillips, C. Lunch, B.J. Bond and M.G. Ryan. 2002*b*. An investigation of hydraulic limitation and compensation in large, old Douglas-fir trees. Tree Physiol. 22:763–774.

Mencuccini, M. and J. Grace. 1996. Hydraulic conductance, light interception and needle nutrient concentration in Scots pine stands and their relations with net primary productivity. Tree Physiol. 16:459–468.

Mencuccini, M., J. Grace and M. Fioravanti. 1997. Biomechanical and hydraulic determinants of tree structure in Scots pine—anatomical characteristics. Tree Physiol. 17:105–113.

Miller, J.M. 2002. Carbon isotope discrimination by *Eucalyptus* species. Ph.D. Thesis, Australian National University, Canberra, 258 p.

Miller, J.M., R.J. Williams and G.D. Farquhar. 2001. Carbon isotope discrimination by a sequence of *Eucalyptus* species along a subcontinental rainfall gradient in Australia. Funct. Ecol. 15: 222–232.

Mokany, K., R.E. McMurtrie, B.J. Atwell and H. Keith. 2003. Interaction between sapwood and foliage area in alpine ash (*Eucalyptus delegatensis*) trees of different heights. Tree Physiol. 23:949–958.

Murty, D., R.E. McMurtrie and M.G. Ryan. 1996. Declining forest productivity in aging forest stands: a modeling analysis of alternative hypotheses. Tree Physiol. 16:187–200.

Obeso, J.R. 2002. The costs of reproduction in plants. New Phytol. 155:321–348.

Phillips, N., B.J. Bond, N.G. McDowell, M.G. Ryan and A. Schauer. 2003. Leaf area compounds height-related hydraulic costs of water transport in Oregon White Oak trees. Funct. Ecol. 17:832–840.

Pothier, D., H.A. Margolis and R.H. Waring. 1989. Patterns of change of saturated sapwood permeability and sapwood conductance with stand development. Can. J. For. Res. 19:432–439.

Ryan, M.G. 1989. Sapwood volume for three subalpine conifers: predictive equations and ecological implications. Can. J. For. Res. 19:1397–1401.

Ryan, M.G. 1991. A simple method for estimating gross carbon budgets for vegetation in forest ecosystems. Tree Physiol. 9:255–266.

Ryan, M.G. and R.H. Waring. 1992. Maintenance respiration and stand development in a subalpine lodgepole pine forest. Ecology 73:2100–2108.

Ryan, M.G. and B.J. Yoder. 1997. Hydraulic limits to tree height and tree growth. Bioscience 47:235–242.

Ryan, M.G., D. Binkley and J. Fownes. 1997. Age-related decline in forest productivity: pattern and process. Adv. Bot. Res. 27: 213–262.

Ryan, M.G., B.J. Bond, B.E. Law, R.M. Hubbard, D. Woodruff, E. Cienciala and J. Kučera. 2000. Transpiration and whole-tree conductance in ponderosa pine trees of different heights. Oecologia 124:553–560.

Saliendra, N.Z., J.S. Sperry and J.P. Comstock. 1995. Influence of leaf water status on stomatal response to humidity, hydraulic conductance, and soil drought in *Betula occidentalis*. Planta 196: 357–366.

Schafer, K.V.R., R. Oren and J.D. Tenhunen. 2000. The effect of tree height on crown level stomatal conductance. Plant Cell Environ. 23:365–375.

Schieving, F. and H. Poorter. 1999. Carbon gain in a multispecies canopy: the role of specific leaf area and photosynthetic nitrogen-use efficiency in the tragedy of the commons. New Phytol. 143: 201–211.

Schoettle, A.W. 1994. Influence of tree size on shoot structure and physiology of *Pinus contorta* and *Pinus aristata*. Tree Physiol. 14:1055–1068.

Schulze, E.D., R.J. Williams, G.D. Farquhar, W. Schulze, J. Langridge, J.M. Miller and B.H. Walker. 1998. Carbon and nitrogen isotope discrimination and nitrogen nutrition of trees along a rainfall gradient in northern Australia. Aust. J. Plant Physiol. 25: 413–425.

Smith, T.M. and M.A. Huston. 1989. A theory of the spatial and temporal dynamics of plant communities. Vegetatio 83:49–69.

Sperry, J.S. 2000. Hydraulic constraints on gas exchange. Agric. For. Meteorol. 104:13–23.

Spicer, R. and B.L. Gartner. 2001. The effects of cambial age and position within the stem on specific conductivity in Douglas-fir (*Pseudotsuga menziesii*) sapwood. Trees 15:222–229.

Vertessy, R.A., R.G. Benyon, S.K. O'Sullivan and P.R. Gribben. 1995. Relationships between stem diameter, sapwood area, leaf area and transpiration in a young mountain ash forest. Tree Physiol. 15:559–567.

Waring, R.H., W.H. Emmingham, H.L. Gholz and C.C. Grier. 1978. Variation in maximum leaf area of coniferous forests in Oregon and its ecological significance. For. Sci. 24:131–140.

Watson, F.G.R., R.A. Vertessy and R.B. Grayson. 1999. Large scale modelling of forest hydrological processes and their long-term effect on water yield. Hydrol. Process. 13:689–700.

Whitehead, D. and P.G. Jarvis. 1981. Coniferous forests and plantations. *In* Water deficits and plant growth. Ed. T.T. Kozlowski. Academic Press, New York, pp 50–132.

Whitehead, D., W.R.N. Edwards and P.G. Jarvis. 1984. Conducting sapwood area, foliage area, and permeability in mature trees of *Picea sitchensis* and *Pinus contorta*. Can. J. For. Res. 14: 940–947.

Williams, M., B.J. Bond and M.G. Ryan. 2001. Evaluating different soil and plant hydraulic constraints on tree function using a model and sap flow data from ponderosa pine. Plant Cell Environ. 24: 679–690.

Yoder, B.J., M.G. Ryan, R.H. Waring, A.W. Schoettle and M.R. Kaufmann. 1994. Evidence of reduced photosynthetic rates in old trees. For. Sci. 40:513–527.

Appendix

Derivation of formal optimality criteria

Whole-tree net carbon (C) gain, A_n, is a function of several C pools, represented by the vector $\mathbf{C} = \langle C_j, ... \rangle$ (where j indicates leaves, fine roots, etc.): $A_n = A_n(\mathbf{C})$. Given a small total increment in structural C, δC_t, available for allocation among these C pools, we wish to maximize the resulting increment in A_n, δA_n. The problem can be solved using Lagrange multipliers. The maximum of a function $f(\mathbf{x})$ subject to a constraint $g(\mathbf{x}) = 0$, occurs at a point $\mathbf{x}_0$ that satisfies:

$$\nabla f(\mathbf{x}_0) = \Omega \nabla g(\mathbf{x}_0) \tag{A1}$$

where Ω is an undetermined constant. For this problem, the vectors $\mathbf{x}$ are sets of allocation fractions, $\mathbf{a} = \langle a_j, ... \rangle$ where $a_j \geq 0$, f is the change in A_n resulting from a partitioned C input of $\mathbf{y} = \delta C_t \mathbf{a}$ (Equation A2), and g is the constraint that the C increments must sum to δC_t (Equation A3):

$$f(\mathbf{a}) = \delta A_n(\mathbf{y}) \tag{A2}$$

$$g(\mathbf{a}) = \mathbf{y} \cdot \mathbf{u} - \delta C_t \equiv 0 \tag{A3}$$

where $\mathbf{u}$ is the unit vector. If f and its derivatives are smooth and continuous, a small change in A_n can be expanded using a Taylor series:

$$\delta A_n = \sum_{k=1}^{\infty} \left(\frac{1}{k!} (\mathbf{y} \cdot \nabla_c)^k A_n \right) = \\ (\mathbf{y} \cdot \nabla_c) A_n + \frac{1}{2} \mathbf{y} \cdot \nabla_c [\mathbf{y} \cdot \nabla_c A_n] + \cdots \tag{A4}$$

where ∇_c denotes a gradient with respect to C pools ($\langle \partial / \partial C_j, ... \rangle$), rather than allocation fractions ($\langle \partial / \partial a_j, ... \rangle$). For vanishingly small δC_t, the second- and higher-order terms become negligible relative to the first-order term, so to a good approximation:

$$\delta A_n \approx (\mathbf{y} \cdot \nabla_c) A_n = \sum_j \delta C_j \frac{\partial A_n}{\partial C_j} = \\ \delta C_t \sum_j a_j \frac{\partial A_n}{\partial C_j} = \delta C_t (\mathbf{a} \cdot \Omega) \tag{A5}$$

where

$$\Omega \equiv \left\langle \frac{\partial A_n}{\partial C_j}, ... \right\rangle$$

optimal allocation vector $\hat{\mathbf{a}} = \langle \hat{a}_j, ... \rangle$, which maximizes the profit from a finite investment of C, is found by applying Equation A1 to Equations A3 and A5. The gradients of f and g are $\nabla f = \delta C_t \langle \Omega_j, ... \rangle$ and $\nabla g = \delta C_t \mathbf{u} = \delta C_t \langle 1, 1, ... \rangle$, so Equation A1 implies:

$$\Omega_j = \Omega \equiv \hat{\Omega} \text{ for all } j \tag{A6}$$

The Lagrange multiplier is implicitly determined by the total resource supply, δC_t. In words, C allocation maximizes C

gain when the marginal gain on C investments is equal for all C pools. This is directly analogous to the optimal solutions for distribution of fixed, finite supplies of water and nitrogen (N) (Cowan and Farquhar 1977, Field 1983, Farquhar 1989, Buckley et al. 2002).

Marginal costs of carbon gain in units of radial sapwood carbon

The marginal gain for radial sapwood C production includes a positive effect (the response of assimilation rate to transpiration rate, E, through conductance) and a negative effect (sapwood maintenance respiration):

$$\frac{1}{1-f_c}\left(\frac{\partial A_n}{\partial C_{sw}}\right)_{H,Z} = L\frac{\partial A}{\partial E}\frac{\partial E}{\partial E_t}\frac{\partial E_t}{\partial S}\frac{\partial S}{\partial C_{sw}} - vn_{sw} = \\ L\frac{1}{\lambda}\frac{1}{L}\frac{\partial E_t}{\partial S}\frac{1}{l\rho_{cw}} - vn_{sw} \quad (A7)$$

where the subscript "H,Z" is omitted for clarity, λ is the marginal cost of C in units of water ($\partial E/\partial A$), l is total axial flow path length and E_t is whole tree transpiration rate (strictly, $\partial S/\partial C_{sw}$ is $1/\rho_{cw}(H + Z + W)$ and l is $H(1 - 0.5LCR) + Z + W$; we ignore this distinction for clarity). The sensitivity of E_t to sapwood area (S) is easily computed by writing E_t as $k_s S\Delta P/(l\eta V_w + k_s S(r_s + r_1))$ where ΔP is $\Psi_s - \rho g_{grav}h - \Psi_1$ (cf. Equation A7 in Buckley and Roberts 2006), differentiating with respect to S and rearranging:

$$\frac{\partial E_t}{\partial S} = \frac{k_s l\Delta P}{(l\eta V_w + k_s S(r_s + r_1))^2} = \\ \frac{E_t}{S}\frac{l\eta V_w}{(l\eta V_w + k_s S(r_s + r_1))} \quad (A8)$$

Applying Equation A8 to Equation A7, noting $E_t = EL$ and rearranging, we have:

$$\frac{1}{1-f_c}\left(\frac{\partial A_n}{\partial C_{sw}}\right)_{H,Z} = \frac{\eta V_w}{\rho_w}\frac{E}{\lambda}\frac{L}{S} \times \\ \frac{1}{(l\cdot\eta V_w + k_s S(r_s + r_1))} - vn_{sw} \quad (A9)$$

For small boundary layer resistance, λ is given by (Buckley et al. 2002):

$$\lambda = \frac{E}{A}\left(1 + \frac{g_s}{g_m}\right) \quad (A10)$$

where g_m is 1.6 times the slope of the biochemical A versus c_i curve, $\partial A/\partial c_i|_{N,I}$, sometimes called mesophyll conductance. Ignoring temperature effects, g_m is determined entirely by photosynthetic capacity, irradiance and stomatal conductance

(g_s) (Buckley et al. 2002). Therefore, $E/\lambda = A/(1 + g_s/g_m)$. Applying this to Equation A9 and rearranging yields:

$$\left(\frac{\partial A_n}{\partial C_{sw}}\right)_{H,Z} \equiv \Omega_{sd} = \\ \left(\left(\frac{L}{S}\right)\frac{\eta V_w}{\rho_{cw}}\left(\frac{A/(1 + g_s/g_m)}{l\eta V_w + k_s S(r_s + r_1)}\right) - vn_{sw}\right)(1 - f_c) \quad (A11)$$

which is Equation 2. The marginal gain from leaf C investment, $\partial A_n/\partial C_1$, is specific leaf area (SLA) times ($\partial A_n/\partial L$). The latter derivative is:

$$\frac{\partial A_n}{\partial L} = (1 - f_c)\frac{\partial}{\partial L}(A_t - v(n_{sw}C_{sw} + n_r C_r + N_t)) \quad (A12)$$

where A_t is annual gross C gain. Of the quantities at right in Equation A12, only A_t is directly affected by L. In turn, A_t depends on L and on the total photosynthetic resource supplies, E_t, N_t, I_t (whole-tree transpiration rate, canopy N content and absorbed photosynthetically active irradiance, respectively). Of these, E_t and I_t depend explicitly on L, but only E_t depends on axial flow path length (l) and L/S. If $r_1 < r_s + r_x$ (where r_x is axial xylem resistance), however, E_t is independent of L, in which case Ω_1 has no explicit dependence on either l or L/S. Then the condition of optimality ($\Omega_1 = \Omega_{sd}$) can be solved directly for L/S as a function of Ω_1 and l, leading to Equation 3.

Effect of senescence rates on L/S

The rate of change of L/S when senescence rates are proportional to pool sizes is:

$$\frac{d}{dt}\left(\frac{L}{S}\right) = \frac{L}{S}\left(\frac{\dot{L}}{L} - \frac{\dot{S}}{S}\right) \approx \frac{L}{S}\left(\frac{\dot{L}^+ - L/\tau_1}{L} - \frac{\dot{S}^+ - S/\tau_{sw}}{S}\right) = \\ \frac{L}{S}\left(\frac{\dot{L}^+}{L} - \frac{\dot{S}^+}{S} - \frac{\tau_{sw} - \tau_1}{\tau_{sw}\tau_1}\right) \quad (A13)$$

where overdots denote time differentiation and $\dot{L}^+$ and $\dot{S}^+$ are the rates of L and S production, respectively. Noting that $S/C_{sw} = (\partial S/\partial C_{sw})_{H,Z}$ (cf. Equation A20 in the accompanying paper, Buckley and Roberts 2006) and $L/C_1 = \partial L/\partial C_1$, the relative production rate for S equals the radial sapwood C production rate ($a_d A_n$) divided by C_{sw}, and similarly $= a_1 A_n/C_1$, so Equation A13 can be rewritten as:

$$\frac{d}{dt}\left(\frac{L}{S}\right) = \frac{L}{S}\left(\frac{a_1 A_n}{C_1} - \frac{a_d A_n}{C_{sw}} - \frac{\tau_{sw} - \tau_1}{\tau_{sw}\tau_1}\right) \quad (A14)$$

which is given as a proportionality in the main text (Equation 4).